

# Metal Nickel Foam as an Efficient and Stable Electrode for Hydrogen Evolution Reaction in Acidic Electrolyte under Reasonable Overpotentials

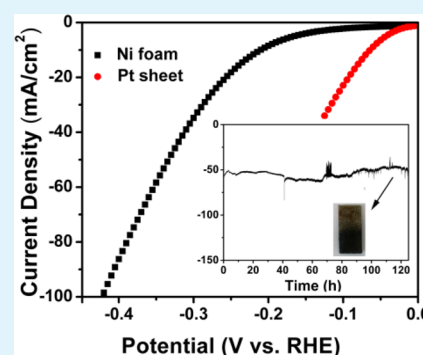
Jia Lu,<sup>†</sup> Tanli Xiong,<sup>†</sup> Weijia Zhou,<sup>\*,†</sup> Linjing Yang,<sup>†</sup> Zhenghua Tang,<sup>†</sup> and Shaowei Chen<sup>\*,†,‡</sup>

<sup>†</sup>New Energy Research Institute, School of Environment and Energy, South China University of Technology, Guangzhou Higher Education Mega Center, Guangzhou, Guangdong 510006, China

<sup>‡</sup>Department of Chemistry and Biochemistry, University of California, 1156 High Street, Santa Cruz, California 95064, United States

## S Supporting Information

**ABSTRACT:** Acidic electrolytes are advantageous for water electrolysis in the production of hydrogen as there is a large supply of H<sup>+</sup> ions in the solution. In this study, with the applied overpotential larger than the equilibrium potential of Ni<sup>0</sup>/Ni<sup>2+</sup>, Ni foam as HER electrode exhibits excellent and stable HER activity with an onset potential of −84 mV (vs RHE), a high current density of 10 mA cm<sup>−2</sup> at −210 mV (vs RHE), and prominent electrochemical durability (longer than 5 days) in acidic electrolyte. The results presented herein may have potential large-scale application in hydrogen energy production.



**KEYWORDS:** stable electrocatalyst, equilibrium potential, hydrogen evolution reaction, nickel foam, acidic electrolyte

Hydrogen has been hailed as a sustainable, secure, and clean alternative energy source that may meet the growing global energy demand. Yet such a perspective is feasible only when hydrogen production can be carried out in an efficient, low-cost, and environmentally friendly fashion. Electrocatalytic hydrogen evolution reaction (HER), preferably driven by solar energy, is a highly attractive means for meeting these requirements.<sup>1–3</sup> Acidic electrolytes (e.g., 0.5 M H<sub>2</sub>SO<sub>4</sub>) are advantageous for water electrolysis in the production of hydrogen as there is a large supply of H<sup>+</sup> ions in the solution. Noble metals such as Pt have been utilized as leading electrocatalysts for HER in acidic electrolytes; however, the scarcity and high cost have limited their widespread applications.<sup>4–6</sup> Therefore, significant research efforts have been devoted to the design and engineering of acid-stable and non-noble catalysts for HER.<sup>7–11</sup>

Molybdenum- and other transition metal-based compounds are an exciting family of catalysts for HER, such as MoS<sub>2</sub>,<sup>12,13</sup> Mo<sub>2</sub>C,<sup>14</sup> MoP,<sup>15</sup> CoSe<sub>2</sub>,<sup>16</sup> and NiP,<sup>17</sup> that exhibit excellent activity and robust stability in acidic electrolytes, as reported in a number of literature studies. However, reports have been scarce where pure transition metals (Co, Fe and Ni, etc.) are used as HER catalysts, because of their chemical instability (corrosion) in acidic environment, except for some metal alloys, such as Ni–Mo<sup>18</sup> and NiMoZn.<sup>19</sup> One typical approach to mitigating the corrosion problem is to deposit a thin carbon layer on the metal surface (metal@carbon). This can not only help protect the transition metals from dissolution in acids but

also promote the catalytic reactions by interfacial charge transfer from the entrapped metal nanoparticles.<sup>20–22</sup> For instance, Zou et al.<sup>21</sup> synthesized cobalt-embedded nitrogen-rich carbon nanotubes (CNTs), and observed apparent electrocatalytic activity for HER, with a small onset potential of −50 mV and a low Tafel slope (69 mV dec<sup>−1</sup>) in 0.5 M H<sub>2</sub>SO<sub>4</sub>. However, the synthetic process was rather complex and tedious. Recently, Tang and Chen reported that single-atom nickel dopants anchored to three-dimensional nanoporous graphene as catalysts for HER in 0.5 M H<sub>2</sub>SO<sub>4</sub> possessed a low overpotential of approximately 50 mV and a Tafel slope of 45 mV dec<sup>−1</sup>, together with excellent cycling stability. Experimental and theoretical investigations suggest that the unusual catalytically active and electrochemically stable performance is due to sp–d orbital charge transfer between the Ni dopants and the surrounding carbon atoms.<sup>23</sup>

Note that Ni is an efficient and stable electrocatalyst in alkaline electrolytes that has been widely used in industrial hydrogen production field.<sup>24,25</sup> However, the high catalytic activity of the nickel-based alloys cannot be sustained in acidic solutions because of Ni dissolution, limiting their applications in feasible and operationally simple electrolytic processes that involve the use of proton-exchange membranes. Is it possible to use pure transition metals, such as Ni, as efficient and stable

Received: January 7, 2016

Accepted: February 17, 2016

Published: February 17, 2016

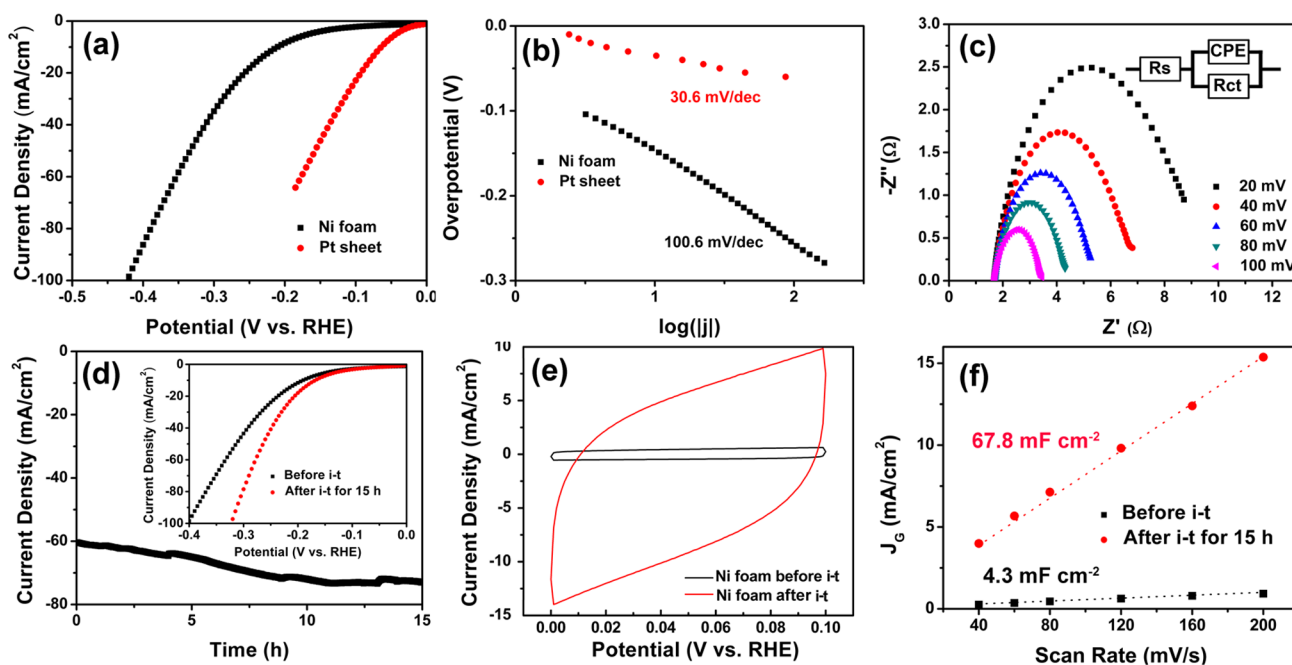
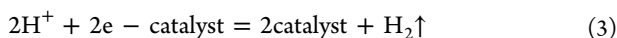
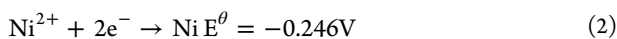
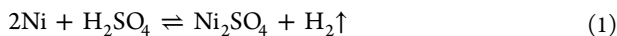


**Figure 1.** (a) Polarization curves for HER in 0.5 M H<sub>2</sub>SO<sub>4</sub> on the Ni foam and platinum foil (Pt). Potential sweep rate is 5 mV s<sup>-1</sup>. (b) Corresponding Tafel plots (overpotential versus log current density with *iR*-correction) derived from panel a. (c) Nyquist plots of Ni foam at various overpotentials in 0.5 M H<sub>2</sub>SO<sub>4</sub>. (d) Current–time plots of Ni foam electrode at the applied potential of –0.43 V (vs RHE). Inset is the polarization curves before and after *i*–*t* testing. (e) Cyclic voltammograms within the range of 0 to +0.1 V where no faradic reactions occurred. (f) Variation in double-layer charging currents at +0.05 V vs RHE with potential scan rate.

electrocatalysts for a long time in acidic electrolyte (e.g., 0.5 M H<sub>2</sub>SO<sub>4</sub>)? Herein, using nickel foam as the example, we examined the feasibility of using pure transition metals as efficient and stable HER catalysts in acidic electrolytes. In acidic electrolyte, nickel metal typically undergoes the following reactions



According to formula 1, the dissolution reaction of nickel in acidic solution is a spontaneous reaction under standard conditions. At the same time, the electrodeposition reactions of Ni<sup>2+</sup> can proceed on the surface of Ni foam electrode according to formula 2. The calculation result showed the electrodeposition voltage should be below –0.246 V (vs RHE), and then the electrodeposition of Ni<sup>2+</sup> can be carried out in formula 2. So, theoretically, the Ni foam as electrode for HER should be stable with an overpotential of > –0.246 V in 0.5 M H<sub>2</sub>SO<sub>4</sub> according to formula 3.

To verify the calculation results, experimentally, we tested the Ni foam as cathode for HER in 0.5 M H<sub>2</sub>SO<sub>4</sub>. As shown in Figure 1a, the polarization curve of Ni foam showed excellent HER activity with an onset potential of –84 mV vs RHE, which was inferior to that of Pt sheet (–18 mV, the calculation method of onset potential as shown in Figure S1). In addition, the Ni foam electrode requires an overpotential of –210 mV to achieve a current density of 10 mA cm<sup>-2</sup>. Furthermore, the linear portions of the polarization curves were fitted to the Tafel equation ( $\eta = b \log j + a$ , where  $j$  is the current density and  $b$  is the Tafel slope), yielding a Tafel slope of 100.6 mV dec<sup>-1</sup> for Ni foam, as compared to 30.6 mV dec<sup>-1</sup> for Pt

(Figure 1b), implying Volmer–Heyrovsky reaction for Ni foam and Tafel reaction for Pt sheet, respectively.

The charge transfer resistance ( $R_{ct}$ ) is related to the electrocatalytic kinetics and its lower value corresponds to the faster reaction rate, which can be obtained from the semicircle in the low frequency zone.  $R_{ct}$  value of Ni foam was found to decrease significantly with increasing overpotentials, from ~7.8 Ω at 20 mV to ~1.9 Ω at 100 mV, suggesting the fast electron transfer and the favorable HER kinetics at the electrolyte interface (Figure 1c).

In addition to good catalytic activity, durability is another important criterion to evaluate the performance of HER electrodes, which is the focus in this work. To verify the stability of Ni foam for HER in 0.5 M H<sub>2</sub>SO<sub>4</sub>, the current–time plots with the applied potential of –0.43 V (vs RHE) were depicted in Figure 1d. The catalytic current increased dramatically from –60 mA cm<sup>-2</sup> to –72.7 mA cm<sup>-2</sup> for 15 h of continuous operation in 0.5 M H<sub>2</sub>SO<sub>4</sub>. Inset of Figure 1d shows that, after *i*–*t* testing for 15 h, the *j*–*V* curve of the Ni foam electrode also increased significantly. It is worth noting that the onset potentials for HER before and after *i*–*t* testing maintained unchanged, which suggested that the catalytic sites of Ni foam did not change, but the effective catalytic area increased.

Typically, the current density is expected to be proportional to catalytically active surface area. One alternative approach to estimate the electrochemical active area is to measure the capacitance of the double layer at the solid–liquid interface with cyclic voltammetry, which were shown in Figure 1e, f. Note that voltammetric study within the potential range of 0 to +0.1 V vs RHE, where no faradic reaction occurred, showed that the double-layer capacitance of the Ni foam electrode increase from 4.3 mF cm<sup>-2</sup> to 67.8 mF cm<sup>-2</sup> after *i*–*t* testing for 15 h, illustrating that the higher catalytic activity of Ni foam

after  $i-t$  testing is attributed to the increased electrochemical surface area. As shown in Figure S2, the  $i-t$  testing of Ni foam as HER electrode in 0.5 M  $\text{H}_2\text{SO}_4$  possessed the constant catalytic current density even up to 5 days (125 h), implying that the Ni foam can be stable for HER in 0.5 M  $\text{H}_2\text{SO}_4$  after the full activation (the increased electrochemical surface area of Ni foam). These superior HER catalytic performance of Ni foam ( $-84$  mV vs RHE, overpotential of  $-210$  mV at the cathodic current density of  $10 \text{ mA cm}^{-2}$ ) is compared favorably to most of the reported values of three-dimensional (3D) nonplatinum HER electrodes in acidic electrolytes (0.5 M  $\text{H}_2\text{SO}_4$ ), such as  $\text{CoS}_2$  nanowire arrays ( $-75$  mV vs RHE,  $51.6 \text{ mV dec}^{-1}$ ,  $10 \text{ mA cm}^{-2}$  at  $-145$  mV),<sup>26</sup>  $\text{MoS}_x$  grown on graphene-protected 3D Ni foam ( $42 \text{ mV dec}^{-1}$ ,  $10 \text{ mA cm}^{-2}$  at  $-151$  mV),<sup>27</sup> 3D  $\text{WS}_2$  nanolayers@heteroatom-doped graphene films ( $10 \text{ mA cm}^{-2}$  at  $-125$  mV),<sup>28</sup> and  $\text{CoSe}_2$  nanoparticles grown on carbon fiber paper ( $10 \text{ mA cm}^{-2}$  at  $-137$  mV),<sup>16</sup> which were summarized in Table S1.

XPS measurements were then conducted to determine the elemental composition and valence state of the Ni foam before and after  $i-t$  testing. As depicted in Figure 2c, d, only the

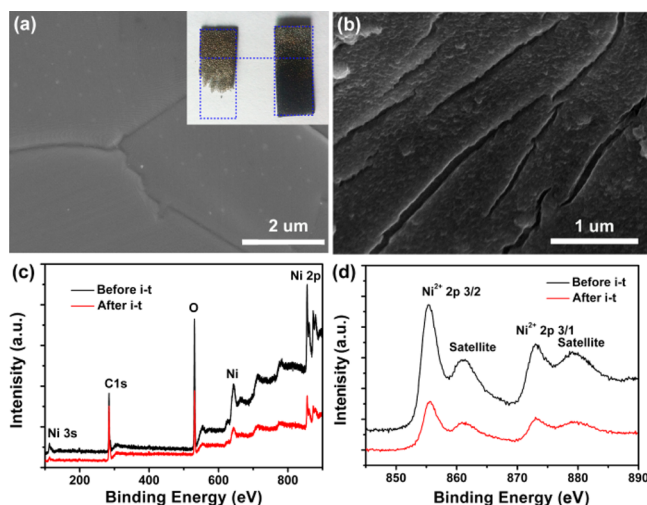


**Figure 2.** (a, b) SEM images and (c, d) XPS survey spectra of Ni foam (a) before and (b) after  $i-t$  testing for 15 h. The inset of images a is the photographs of Ni foam: the left is Ni foam dipped in 0.5 M  $\text{H}_2\text{SO}_4$  solution for 15 h; the right is Ni foam after  $i-t$  testing at  $-0.43$  V vs RHE in 0.5 M  $\text{H}_2\text{SO}_4$  for 15 h.

elements of Ni, O, and C (from conductive carbon tape) can be identified for both samples. In comparison with the pure Ni foam, there are no new elements in the black Ni foam after  $i-t$  testing. Deconvolution of the high-resolution scan of the Ni 2p electrons yielded two peaks at 855.5 and 873.1 eV (Figure 2d), which represent the characteristic Ni 2p<sub>3/2</sub> and Ni 2p<sub>1/2</sub> peaks of Ni 2p, respectively.<sup>11,29</sup> In addition, XRD results of Ni foam before and after  $i-t$  testing also confirmed that no impurity was detected (Figure S3), only peaks of Ni were detected (JCPDS no.65-2865). Transmission electron microscopy (TEM) images of Ni foam after  $i-t$  testing were shown in Figure S4, there are two different lattice fringes of 0.204 and 0.176 nm, corresponding to the (111) plane and (200) plane of Ni, respectively. All these results fully validated that the formation of blackened Ni foam after  $i-t$  testing was attributed to the appearance of rough surface, not to the change of the elemental composition and valence states. These results further confirm

that the pure Ni metal possessed the efficient HER activity in acidic electrolyte.

The impacts of the metal elements on the activity and stability for HER in acid electrolyte were examined and compared, including Al, Fe, and Ti sheets with same geometric area. From Figure 3a, apparent nonzero cathodic currents can

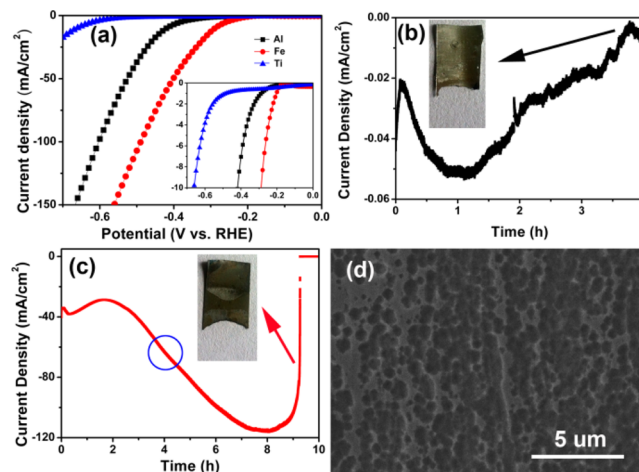


**Figure 3.** (a) Polarization curves for HER in 0.5 M  $\text{H}_2\text{SO}_4$  at different metal electrodes, including Al, Fe, and Ti, respectively. Current-time plots of (b) Al and (c) Fe electrodes at the applied potential of  $-0.43$  V (vs RHE). (d) SEM image of Fe sheet after  $i-t$  testing for 4 h.

be seen at all the metal electrodes, however, remarkably different HER activities can be easily recognized. The overpotential of Fe sheet at a current density of  $10 \text{ mA cm}^{-2}$  was the lowest ( $-288$  mV vs RHE) among the series, which increased in the order of Fe ( $-288$  mV), Al ( $-419$  mV), and Ti ( $-660$  mV). In fact, metal Fe as core protected by carbon shell from dissolution in acidic electrolyte has been reported as efficient and stable electrocatalysts in 0.5 M  $\text{H}_2\text{SO}_4$ .<sup>22,30</sup> However, herein, Fe and Al without carbon shell as electrodes were dissolved into 0.5 M  $\text{H}_2\text{SO}_4$ , even with high applied overpotential ( $-0.43$  V vs RHE), excepting for Ti with Antiacid corrosion. In Figure 3b, c, the current densities first increased, and then sharply reduced until to zero in short time, 4 h for Al electrode and 10 h for Fe electrode, respectively. In Figure 3d, the surface of Fe electrode after 4 h of  $i-t$  testing became rough due to acid corrosion. Inset of Figure 3b, c showed the photos of broken electrodes of Al and Fe, implying the unstable reaction for HER. The reasons of the different HER stabilities in 0.5 M  $\text{H}_2\text{SO}_4$  among Ni, Al and Fe were discussed. On the basis of the above mechanism, Ni foam as cathode for HER should be stable with an overpotential ( $-0.43$  V vs RHE) greater than equilibrium potential of Ni ( $-0.246$  V vs RHE) in 0.5 M  $\text{H}_2\text{SO}_4$ . But, the equilibrium potentials of Fe ( $E^\theta = -0.44$  V) and Al ( $E^\theta = -1.66$  V) were higher than the applied overpotential of  $-0.43$  V (vs RHE), leading to the unstable catalytic reaction in 0.5 M  $\text{H}_2\text{SO}_4$  for Al and Fe electrodes. To confirm the speculation, we applied an overpotential of 0.23 V for Ni foam electrode, and the decreased current density was observed, implying the unstable catalytic reaction in 0.5 M  $\text{H}_2\text{SO}_4$  (Figure S5). So, herein, Ni foam was proven as efficient and relatively stable HER electrocatalyst applied an appropriate overpotential in acidic electrolyte. What's more, the equilibrium relationship among electrocatalytic hydrogen production, electrodeposition, and corrosion of transition metals gave the

guidance in catalytic reaction on the surface of electrode in acid electrolyte.

In this study, we found that the transition metals, specifically Ni foam, can be employed as efficient and relatively stable electrocatalyst for HER in acidic electrolyte. Electrochemical testing showed that pure Ni foam electrode exhibited excellent and stable HER activity of an onset potential of  $-84$  mV (vs RHE), a high current density of  $10$  mA cm $^{-2}$  at  $-210$  mV (vs RHE), and Tafel slope of  $100.6$  mV dec $^{-1}$ . It is worth noting that Ni foam possess the prominent electrochemical durability (longer than 5 days) during the HER in acidic electrolyte ( $0.5$  M H $_2$ SO $_4$ ) with the applied overpotential larger than the equilibrium potential of Ni ( $-0.246$  V vs RHE). SEM and XPS results confirmed that the elemental composition and valence states of Ni foam have no change after  $i-t$  testing for 15 h. The results presented herein may offer a new electrochemical methodology to obtain effective and stable HER activity of pure transition metals in acidic electrolyte, which has potential large-scale application in hydrogen energy production.

## ■ ASSOCIATED CONTENT

### Supporting Information

This material is available free of charge on the ACS Publications Web site at The Supporting Information is available free of charge on the ACS Publications website at DOI: 10.1021/acsami.6b00233.

Experimental section, comparison of HER performance among Ni foam electrode and reported 3D electrodes, polarization curves for HER in  $0.5$  M H $_2$ SO $_4$  on the Ni foam and platinum foil (Pt), XRD patterns and TEM images of Ni foam, current–time plots of the Ni foam electrode (PDF)

## ■ AUTHOR INFORMATION

### Corresponding Authors

\*E-mail: eszhouwj@scut.edu.cn.

\*E-mail: shaowei@ucsc.edu.

### Notes

The authors declare no competing financial interest.

## ■ ACKNOWLEDGMENTS

This work was supported by the National Recruitment Program of Global Experts, Zhujiang New Stars of Science & Technology (2014J2200061), Project of Public Interest Research and Capacity Building of Guangdong Province (2014A010106005), the Fundamental Research Funds for the Central Universities (D2153880), and the National Natural Science Foundation of China (51502096).

## ■ REFERENCES

- (1) Luo, J.; Im, J.-H.; Mayer, M. T.; Schreier, M.; Nazeeruddin, M. K.; Park, N.-G.; Tilley, S. D.; Fan, H. J.; Grätzel, M. Water Photolysis at 12.3% Efficiency Via Perovskite Photovoltaics and Earth-Abundant Catalysts. *Science* **2014**, *345*, 1593–1596.
- (2) Yang, J.; Shin, H. S. Recent Advances in Layered Transition Metal Dichalcogenides for Hydrogen Evolution Reaction. *J. Mater. Chem. A* **2014**, *2*, 5979–5985.
- (3) Zhou, W.; Wu, X.-J.; Cao, X.; Huang, X.; Tan, C.; Tian, J.; Liu, H.; Wang, J.; Zhang, H. Ni $_3$ S $_2$  Nanorods/Ni Foam Composite Electrode with Low Overpotential for Electrocatalytic Oxygen Evolution. *Energy Environ. Sci.* **2013**, *6*, 2921–2924.
- (4) Deng, J.; Li, H.; Xiao, J.; Tu, Y.; Deng, D.; Yang, H.; Tian, H.; Li, J.; Ren, P.; Bao, X. Triggering the Electrocatalytic Hydrogen Evolution

Activity of the Inert Two-Dimensional MoS $_2$  Surface Via Single-Atom Metal Doping. *Energy Environ. Sci.* **2015**, *8*, 1594–1601.

(5) Bai, S.; Wang, C.; Deng, M.; Gong, M.; Bai, Y.; Jiang, J.; Xiong, Y. Surface Polarization Matters: Enhancing the Hydrogen-Evolution Reaction by Shrinking Pt Shells in Pt–Pd–Graphene Stack Structures. *Angew. Chem., Int. Ed.* **2014**, *53*, 12120–12124.

(6) Hou, D.; Zhou, W.; Liu, X.; Zhou, K.; Xie, J.; Li, G.; Chen, S. Pt Nanoparticles/MoS $_2$  Nanosheets/Carbon Fibers as Efficient Catalyst for the Hydrogen Evolution Reaction. *Electrochim. Acta* **2015**, *166*, 26–31.

(7) Zhou, Y.; Leng, Y.; Zhou, W.; Huang, J.; Zhao, M.; Zhan, J.; Feng, C.; Tang, Z.; Chen, S.; Liu, H. Sulfur and Nitrogen Self-Doped Carbon Nanosheets Derived from Peanut Root Nodules as High-Efficiency Non-Metal Electrocatalyst for Hydrogen Evolution Reaction. *Nano Energy* **2015**, *16*, 357–366.

(8) Hou, D.; Zhou, W.; Zhou, K.; Zhou, Y.; Zhong, J.; Yang, L.; Lu, J.; Li, G.; Chen, S. Flexible and Porous Catalyst Electrodes Constructed by Co Nanoparticles@Nitrogen-Doped Graphene Films for Highly Efficient Hydrogen Evolution. *J. Mater. Chem. A* **2015**, *3*, 15962–15968.

(9) Hou, Y.; Wen, Z.; Cui, S.; Ci, S.; Mao, S.; Chen, J. An Advanced Nitrogen-Doped Graphene/Cobalt-Embedded Porous Carbon Polyhedron Hybrid for Efficient Catalysis of Oxygen Reduction and Water Splitting. *Adv. Funct. Mater.* **2015**, *25*, 872–882.

(10) Zhou, W.; Zhou, J.; Zhou, Y.; Lu, J.; Zhou, K.; Yang, L.; Tang, Z.; Li, L.; Chen, S. N-Doped Carbon-Wrapped Cobalt Nanoparticles on N-Doped Graphene Nanosheets for High-Efficiency Hydrogen Production. *Chem. Mater.* **2015**, *27*, 2026–2032.

(11) Gong, M.; Zhou, W.; Tsai, M.-C.; Zhou, J.; Guan, M.; Lin, M.-C.; Zhang, B.; Hu, Y.; Wang, D.-Y.; Yang, J. Nanoscale Nickel Oxide/Nickel Heterostructures for Active Hydrogen Evolution Electrocatalysis. *Nat. Commun.* **2014**, *5*, 4695.

(12) Zhou, W.; Zhou, K.; Hou, D.; Liu, X.; Li, G.; Sang, Y.; Liu, H.; Li, L.; Chen, S. Three-Dimensional Hierarchical Frameworks Based on MoS $_2$  Nanosheets Self-Assembled on Graphene Oxide for Efficient Electrocatalytic Hydrogen Evolution. *ACS Appl. Mater. Interfaces* **2014**, *6*, 21534–21540.

(13) Gopalakrishnan, D.; Damien, D.; Shajumon, M. M. MoS $_2$  Quantum Dot-Interspersed Exfoliated MoS $_2$  Nanosheets. *ACS Nano* **2014**, *8*, 5297–5303.

(14) Wu, H. B.; Xia, B. Y.; Yu, L.; Yu, X.-Y.; Lou, X. W. D. Porous Molybdenum Carbide Nano-Octahedrons Synthesized Via Confined Carburization in Metal-Organic Frameworks for Efficient Hydrogen Production. *Nat. Commun.* **2015**, *6*, 6512.

(15) Xing, Z.; Liu, Q.; Asiri, A. M.; Sun, X. Closely Interconnected Network of Molybdenum Phosphide Nanoparticles: A Highly Efficient Electrocatalyst for Generating Hydrogen from Water. *Adv. Mater.* **2014**, *26*, 5702–5707.

(16) Kong, D.; Wang, H.; Lu, Z.; Cui, Y. CoSe $_2$  Nanoparticles Grown on Carbon Fiber Paper: An Efficient and Stable Electrocatalyst for Hydrogen Evolution Reaction. *J. Am. Chem. Soc.* **2014**, *136*, 4897–4900.

(17) Popczun, E. J.; McKone, J. R.; Read, C. G.; Biacchi, A. J.; Wiltrout, A. M.; Lewis, N. S.; Schaak, R. E. Nanostructured Nickel Phosphide as an Electrocatalyst for the Hydrogen Evolution Reaction. *J. Am. Chem. Soc.* **2013**, *135*, 9267–9270.

(18) McKone, J. R.; Sadtler, B. F.; Werlang, C. A.; Lewis, N. S.; Gray, H. B. Ni–Mo Nanopowders for Efficient Electrochemical Hydrogen Evolution. *ACS Catal.* **2013**, *3*, 166–169.

(19) Wang, F.; Li, J.; Wang, F.; Shifa, T. A.; Cheng, Z.; Wang, Z.; Xu, K.; Zhan, X.; Wang, Q.; Huang, Y.; Jiang, C.; He, J. Enhanced Electrochemical H $_2$  Evolution by Few-Layered Metallic WS $_2$ ( $1-x$ )Se $_{2x}$  Nanoribbons. *Adv. Funct. Mater.* **2015**, *25*, 6077–6083.

(20) Zhou, W.; Zhou, Y.; Yang, L.; Huang, J.; Ke, Y.; Zhou, K.; Li, L.; Chen, S. N-Doped Carbon-Coated Cobalt Nanorod Arrays Supported on a Titanium Mesh as Highly Active Electrocatalysts for the Hydrogen Evolution Reaction. *J. Mater. Chem. A* **2015**, *3*, 1915–1919.

(21) Zou, X.; Huang, X.; Goswami, A.; Silva, R.; Sathe, B. R.; Mikmeková, E.; Asefa, T. Cobalt-Embedded Nitrogen-Rich Carbon

Nanotubes Efficiently Catalyze Hydrogen Evolution Reaction at All PH Values. *Angew. Chem.* **2014**, *126*, 4461–4465.

(22) Deng, J.; Ren, P.; Deng, D.; Bao, X. Enhanced Electron Penetration through an Ultrathin Graphene Layer for Highly Efficient Catalysis of the Hydrogen Evolution Reaction. *Angew. Chem., Int. Ed.* **2015**, *54*, 2100–2104.

(23) Qiu, H. J.; Ito, Y.; Cong, W.; Tan, Y.; Liu, P.; Hirata, A.; Fujita, T.; Tang, Z.; Chen, M. Nanoporous Graphene with Single-Atom Nickel Dopants: An Efficient and Stable Catalyst for Electrochemical Hydrogen Production. *Angew. Chem.* **2015**, *127*, 14237–14241.

(24) Yu, X.; Hua, T.; Liu, X.; Yan, Z.; Xu, P.; Du, P. Nickel-Based Thin Film on Multiwalled Carbon Nanotubes as an Efficient Bifunctional Electrocatalyst for Water Splitting. *ACS Appl. Mater. Interfaces* **2014**, *6*, 15395–15402.

(25) Peng, Z.; Jia, D.; Al-Enizi, A. M.; Elzatahry, A. A.; Zheng, G. From Water Oxidation to Reduction: Homologous Ni–Co Based Nanowires as Complementary Water Splitting Electrocatalysts. *Adv. Energy Mater.* **2015**, *5*, 1402031.

(26) Faber, M. S.; Dziedzic, R.; Lukowski, M. A.; Kaiser, N. S.; Ding, Q.; Jin, S. High-Performance Electrocatalysis Using Metallic Cobalt Pyrite (CoS<sub>2</sub>) Micro- and Nanostructures. *J. Am. Chem. Soc.* **2014**, *136*, 10053–10061.

(27) Chang, Y. H.; Lin, C. T.; Chen, T. Y.; Hsu, C. L.; Lee, Y. H.; Zhang, W.; Wei, K. H.; Li, L. J. Highly Efficient Electrocatalytic Hydrogen Production by MoS<sub>x</sub> Grown on Graphene-Protected 3d Ni Foams. *Adv. Mater.* **2013**, *25*, 756–760.

(28) Duan, J.; Chen, S.; Chambers, B. A.; Andersson, G. G.; Qiao, S. Z. 3D WS<sub>2</sub> Nanolayers@ Heteroatom-Doped Graphene Films as Hydrogen Evolution Catalyst Electrodes. *Adv. Mater.* **2015**, *27*, 4234–4241.

(29) Yu, M.; Wang, W.; Li, C.; Zhai, T.; Lu, X.; Tong, Y. Scalable Self-Growth of Ni@NiO Core-Shell Electrode with Ultrahigh Capacitance and Super-Long Cyclic Stability for Supercapacitors. *NPG Asia Mater.* **2014**, *6*, e129.

(30) Tavakkoli, M.; Kallio, T.; Reynaud, O.; Nasibulin, A. G.; Johans, C.; Sainio, J.; Jiang, H.; Kauppinen, E. I.; Laasonen, K. Single-Shell Carbon-Encapsulated Iron Nanoparticles: Synthesis and High Electrocatalytic Activity for Hydrogen Evolution Reaction. *Angew. Chem.* **2015**, *127*, 4618–4621.